Correlation of FDG-PET findings with histopathology in the assessment of response to induction chemoradiotherapy in non-small cell lung cancer

Yuka Yamamoto[1], Yoshihiro Nishiyama[1], Toshihide Monden[1], Yasuhiro Sasakawa[1], Motoomi Ohkawa[1], Masashi Gotoh[2], Kotaro Kameyama[2], Reiji Haba[3]

[1] Faculty of Medicine, Department of Radiology, Kagawa University, Kita-gun, Kagawa, Japan
[2] Faculty of Medicine, Department of Second Surgery, Kagawa University, Kita-gun, Kagawa, Japan
[3] Faculty of Medicine, Department of Diagnostic Pathology, Kagawa University, Kita-gun, Kagawa, Japan

Abstract. *Purpose:* The objective of this study was to evaluate the ability of FDG-PET to predict the response of primary tumour and nodal disease to preoperative induction chemoradiotherapy in patients with non-small cell lung cancer (NSCLC).
Methods: FDG-PET studies were performed before and after completion of chemoradiotherapy prior to surgery in 26 patients with NSCLC. FDG-PET imaging was performed at 1 h (early) and 2 h (delayed) after injection. Semi-quantitative analysis was performed using the standardised uptake value (SUV) at the primary tumour. Percent change was calculated according to the following equation: $(SUV_{after} - SUV_{before}) \times 100/SUV_{before}$. Based on histopathological analysis of the specimens obtained at surgery, patients were classified as pathological responders or pathological non-responders. The clinical nodal stage on the post-chemoradiotherapy PET scan was visually determined and compared with the final pathological stage.
Results: Eighteen patients were found to be pathological responders and eight to be pathological non-responders. SUV_{after} values from both early and delayed images in pathological responders were significantly lower than those in pathological non-responders. The percent change values from early and delayed images in the pathological responders were significantly higher than those in the pathological non-responders. The post-chemoradiotherapy PET scan accurately predicted nodal stage in 22 of 26 patients.
Conclusion: FDG-PET may have the potential to predict response to induction chemoradiotherapy in patients with NSCLC.

Yuka Yamamoto (✉)
Faculty of Medicine, Department of Radiology,
Kagawa University,
Kita-gun,
Kagawa, Japan
e-mail: yuka@kms.ac.jp

Introduction

Non-small cell lung cancer (NSCLC) is one of the most important causes of cancer-related deaths world-wide [1]. Use of a multimodality approach including preoperative chemoradiotherapy has led to a substantial improvement in survival in patients with locally advanced NSCLC [2]. Complete pathological response to neoadjuvant chemotherapy and radiotherapy is an important prognostic indicator for prolonged disease-free survival. An accurate assessment of the impact of chemo- and/or radiotherapy would help in assessing treatment for patients with locally advanced NSCLC. Presently, effectiveness of therapy is evaluated using morphological changes as assessed by anatomical imaging techniques such as computed tomography (CT) and magnetic resonance imaging (MRI). These techniques rely on changes in tumour size to assess tumour response. However, it may take weeks or even months to know the success or failure of chemoradiotherapy [3]. Furthermore, it is difficult to distinguish residual tumour from necrosis or fibrosis [4]. Techniques that image function rather than anatomy might overcome these drawbacks and provide better accuracy in monitoring response, given that functional changes are expected to precede morphological changes.

Positron emission tomography (PET) scanning with [^{18}F]-2-fluoro-2-deoxy-D-glucose (FDG) has shown substantial promise during the past decade in aiding in the non-invasive preoperative staging of lung cancer [5, 6]. FDG-PET imaging uses the radiolabelled FDG tracer as a glucose ana-

logue with comparable uptake in metabolically active cells. Accumulation of FDG is greater in metabolically active tumour than in necrotic tissue. The role of FDG-PET in restaging patients with NSCLC after neoadjuvant therapy has not been fully investigated [7, 8]. It is anticipated that such biochemical changes will occur much sooner than changes in tumour size. Such a change in the metabolic status may be an early biochemical marker for subsequent histopathological tumour response.

At the same time, however, FDG also accumulates in inflammatory processes reactive to treatment, and this has especially been observed after radiotherapy [7, 9]. PET study protocols usually entail imaging at 1 h after FDG administration. In animal experiments, FDG accumulation by tumours was found to constantly increase over 2 or 3 h [10]. Conversely, Yamada et al. [11] reported that FDG uptake in inflammatory lesions showed a peak at approximately 1 h after injection. Some human studies have demonstrated that delayed FDG-PET scanning may help to differentiate malignant solitary pulmonary nodules from benign ones [12–14].

In the present study, we evaluated the ability of FDG-PET scanning to predict the response of both primary tumours and nodal disease to preoperative induction chemoradiotherapy in NSCLC. The change in PET activity after chemoradiotherapy was measured and correlated with pathological response. Because there is currently no consensus as to the best time of data acquisition for monitoring PET activity, we compared early and delayed PET images with respect to their ability to predict response to chemoradiotherapy.

Materials and methods

Patients

Twenty-six patients with locally advanced NSCLC who received preoperative induction chemoradiotherapy were included in the study. They included 22 males and 4 females with a mean age of 65.2 years (range 51–76 years). Of the patients, 17 had clinical stage IIIA (T1N2, 6; T2N2, 8; T3N1, 1; T3N2, 2) and nine, clinical stage IIIB (T3N3, 1; T4N0, 3; T4N1, 3; T4N2, 2). Histological types of tumour were squamous cell carcinoma in 14 and adenocarcinoma in 12. None of the patients were assessed for nodal stage with mediastinoscopy before treatment. This study was approved by the local ethics committee, and all patients provided written or oral informed consent.

Preoperative therapy

The treatment plan consisted of preoperative concurrent chemoradiotherapy and surgery. The preoperative radiotherapy consisted of 40–50 Gy in 2-Gy fractions, with five fractions given weekly using the 10-MV beam of a MEVATRON KD2/50 PRIMUS (Toshiba, Tokyo, Japan) linear accelerator. The target volume included the primary tumour, clinically involved mediastinal and hilar nodes, and adjacent uninvolved ipsilateral mediastinal and hilar nodes for CT-based treatment planning.

Patients received two cycles of chemotherapy during the radiotherapy period. The first cycle of chemotherapy was applied on the next day after the start of the radiotherapy. The second cycle of chemotherapy was applied 4 weeks after the first cycle. The chemotherapy regimen was carboplatin/paclitaxel in 11 patients and carboplatin/docetaxel in 15. Carboplatin [area under the curve (AUC) 6 mg/ml × min] on day 1 and paclitaxel at 180 mg/m^2 body surface area (BSA) on day 1 or docetaxel at 60 mg/m^{2}BSA on day 1 were administered.

Patients who remained free of distant metastasis underwent thoracotomy 6–8 weeks after completion of preoperative chemoradiotherapy.

FDG-PET image acquisition and reconstruction

Patients had FDG-PET scans before the initiation and 3–4 weeks after completion of preoperative induction chemoradiotherapy. Patients were instructed to fast for at least 5 h prior to PET imaging. None of the patients had a history of diabetes. Accordingly, no intravenous insulin was administered.

All FDG-PET examinations were performed with an ECAT EXACT HR+ (Siemens/CTI Inc., Knoxville, TN). This camera acquires 63 planes simultaneously over a 15.5-cm field of view. In-plane resolution is approximately 4.6 mm, with an axial resolution of approximately 3.5 mm full-width at half-maximum. Images were acquired in 3D mode. Transmission scan was obtained using a ^{68}Ge rod source for the purpose of attenuation correction. Image reconstruction was performed with accelerated maximum likelihood reconstruction and ordered-subset expectation maximisation, which reduces image noise and avoids reconstruction artefacts resulting from filtered backprojection reconstruction of data with low count densities. Radiochemical purity, sterility and pyrogenicity of FDG were tested for each sample at our cyclotron unit.

Image acquisition for the whole-body scan started at 60 min after the injection of 3 MBq/kg FDG. This first scan (early image) included the skull base, neck, thorax, abdomen and pelvis. Six or seven bed positions were used to scan from the skull base to the upper thighs. After an interval of 60 min, a second scan of the thorax only (delayed image) was acquired in all patients. Starting at the same position as for the early scan, the delayed scan covered an axial length of 25.6–38.4 cm involving two or three bed positions.

PET image interpretation and data analysis

Both early and delayed PET images were evaluated semiquantitatively by standardised uptake value (SUV) analysis. SUV was measured in the primary tumour before and after chemoradiotherapy. It was defined as the tissue concentration of FDG (kBq/ml) in the structure delineated by the region of interest (ROI) divided by the activity injected per gram body weight (kBq/g). An ROI was placed over the entire primary tumour. The maximum SUV of the primary tumour was used. When little or no tumour-related radioactivity was discernible by visual analysis (post-therapy studies), the ROI was positioned on the basis of CT data and pre-therapy FDG-PET data. We called the SUV of images obtained before therapy "SUV$_{before}$" and the SUV of images obtained after therapy "SUV$_{after}$". Furthermore, percent change was calculated from SUV$_{before}$ and SUV$_{after}$ as follows: $(SUV_{after} - SUV_{before}) \times 100/SUV_{before}$.

All surgical resection specimens obtained after completion of chemoradiotherapy were evaluated by a pathologist in order to determine the degree of pathological tumour response. Pathological primary tumour response to induction chemoradiotherapy was classified as pathological response or pathological non-response. A pathological responder was defined as a patient with either no tumour

Table 1. Assessment of SUV results on FDG-PET scans before and after induction chemoradiotherapy, according to the pathological response in 26 patients with NSCLC

	SUV_{before}		SUV_{after}	
	Early image	Delayed image	Early image	Delayed image
Pathological responders (n=18)	11.5±6.1	14.9±8.4	2.6±1.0*, $	2.7±1.4*, $$
Squamous cell carcinoma (n=12)	11.0±6.7	14.4±9.2	2.4±1.0**, $$$	2.5±1.2**, $$$
Adenocarcinoma (n=6)	12.3±4.9	15.9±7.4	2.9±1.1***, $	3.2±1.6***
Pathological non-responders (n=8)	14.3±5.9	20.0±10.3	6.0±2.1+	7.4±2.9+
Squamous cell carcinoma (n=2)	13.0±2.2	19.5±2.9	5.8±0.1	7.9±0.7
Adenocarcinoma (n=6)	14.7±6.9	20.2±12.1	6.0±2.5++	7.3±3.5++

Data are given as mean±standard deviation

SUV_{before} standardised uptake value of before therapy, SUV_{after} standardised uptake value of after therapy

*P=0.0002, **P=0.002 and ***P=0.03 compared with the corresponding SUV_{before} in pathological responders

[+] P=0.02 and [++] P=0.03 compared with the corresponding SUV_{before} in pathological non-responders

$ P=0.0005, $$ P=0.0015 and $$$ P=0.03 compared with the corresponding SUV_{after} in pathological non-responders

(complete response) or residual microscopic disease only. A pathological non-responder was defined as a patient with residual macroscopic disease.

The clinical nodal stage from the post-chemoradiotherapy PET scan was also determined and compared with the final pathological stage. SUV was not determined for lymph nodes because their small and irregular size resulted in underestimation of total ^{18}F uptake (limited count recovery due to PET scanner resolution and partial volume effects). For evaluation of mediastinal and hilar lymph nodes, focal areas of uptake with an intensity greater than non-cardiac mediastinal structures were considered to represent nodal metastasis. Individual nodal groups were characterised according to the modified AJCC classifications [15].

Statistical analysis

Differences in semi-quantitative parameters were analysed by the Mann-Whitney U test and the Wilcoxon signed rank test for unpaired and paired observations, respectively. For calculation of sensitivity and specificity, the optimal SUV and percent change cut-off for differentiating between pathological responders and non-responders was chosen retrospectively to yield the lowest number of false-
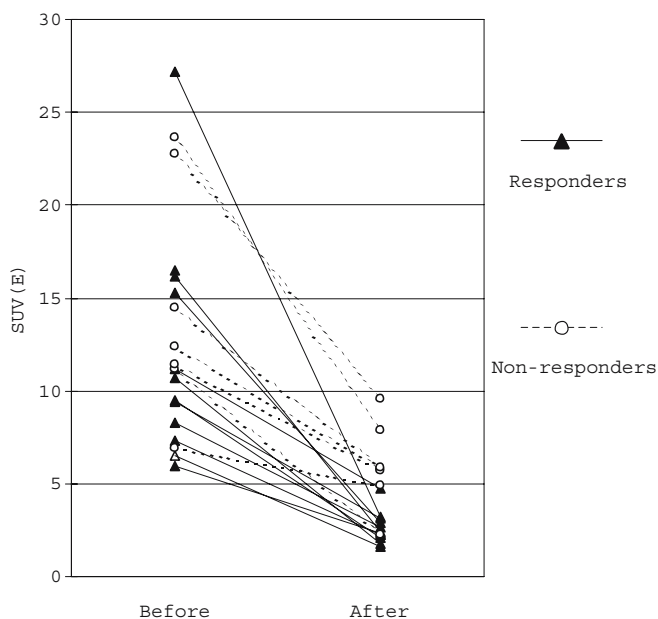

Fig. 1. Change in SUV on early FDG-PET images (*SUV (E)*) after chemoradiotherapy, according to the pathological response in 26 patients with NSCLC
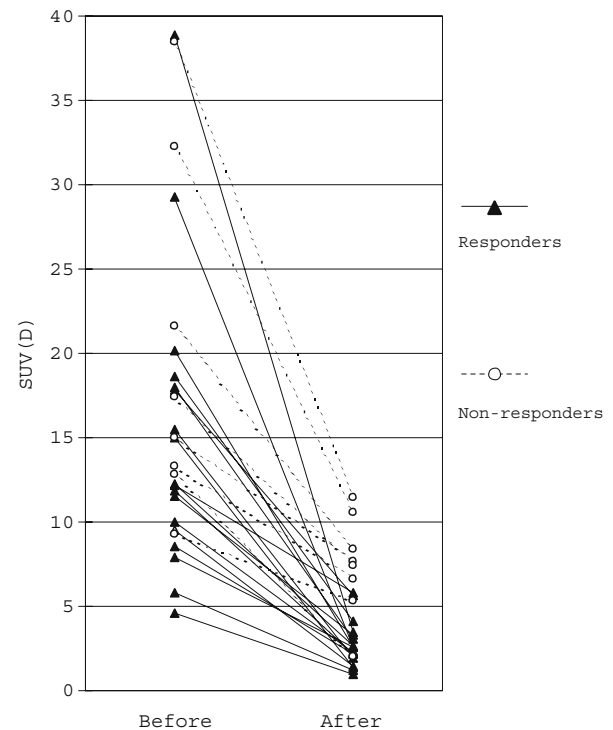

Fig. 2. Change in SUV on delayed FDG-PET images (*SUV (D)*) after chemoradiotherapy, according to the pathological response in 26 patients with NSCLC

Table 2. Percent change values in FDG-PET scans according to the pathological response in 26 patients with NSCLC

	Early image	Delayed image
Pathological responders (n=18)	74.1±10.1*	79.1±10.0**
Squamous cell carcinoma (n=12)	74.2±9.8***	80.4±7.2***
Adenocarcinoma (n=6)	73.9±11.5	76.4±14.7
Pathological non-responders (n=8)	55.5±14.8	60.2±13.5
Squamous cell carcinoma (n=2)	54.6±6.9	59.4±2.8
Adenocarcinoma (n=6)	55.9±17.2	60.5±16.0

Data are given as mean±standard deviation
*P=0.003, **P=0.004 and ***P=0.03 compared with the corresponding pathological non-responders

negative and false-positive results. All semi-quantitative data were expressed as mean±SD. Results were considered significant when $p<0.05$.

Results

All patients remained free of distant metastasis and underwent thoracotomy after completion of preoperative chemoradiotherapy with the aim of complete resection of the primary lesion and ipsilateral mediastinal and hilar lymph nodes. The median time interval between the completion of the chemoradiotherapy and the second (after chemoradiotherapy) FDG-PET scan was 19.3 days (range 3–57 days). The median time interval between the completion of the chemoradiotherapy and the surgery was 48.0 days (range 20–102 days). Eighteen patients were considered pathological responders (complete response, 4; residual microscopic disease, 14) and eight, pathological non-responders (residual macroscopic disease).

Assessment of primary tumour before and after chemoradiotherapy

Before therapy, all 26 primary tumours showed intense uptake greater than that in non-cardiac mediastinal
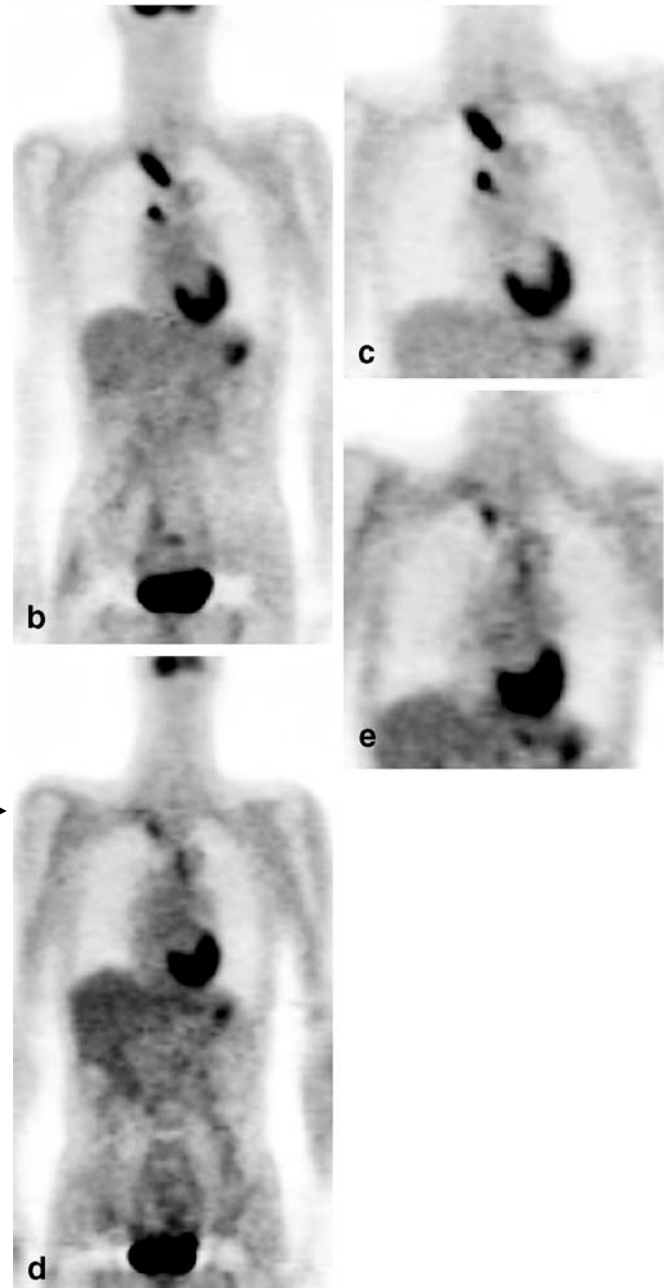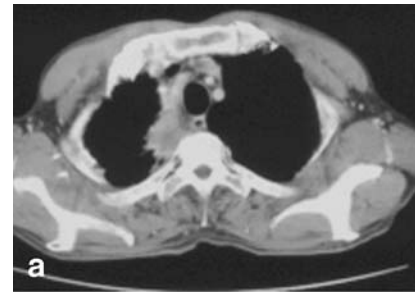

Fig. 3. CT and FDG-PET images of a 60-year-old male pathological responder (residual microscopic disease) with squamous cell carcinoma in the right upper lobe. CT image before therapy shows a mass shadow in the right upper lobe (**a**). Both early (**b**) and delayed (**c**) FDG-PET coronal images before therapy show intense accumulation in both the primary tumour and an ipsilateral mediastinal lymph node. On early and delayed images, SUVs for the primary tumour were 8.27 and 12.27, respectively. After chemoradiotherapy, the intense accumulation in the primary tumour was decreased on both early (**d**) and delayed (**e**) FDG-PET coronal images: on early and delayed images, SUVs for the primary tumour were 2.68 and 2.70, respectively. The percent change values in respect of the primary tumour on early and delayed images were 67.6 and 78.0, respectively. No abnormal accumulation was seen in the ipsilateral mediastinal lymph node (**d**, **e**) after chemoradiotherapy. The longitudinal faint accumulation in the mediastinal structure is due to radiation oesophagitis. Nodal stage based on early and delayed FDG-PET images after chemoradiotherapy was N0 and pathological nodal stage was N0
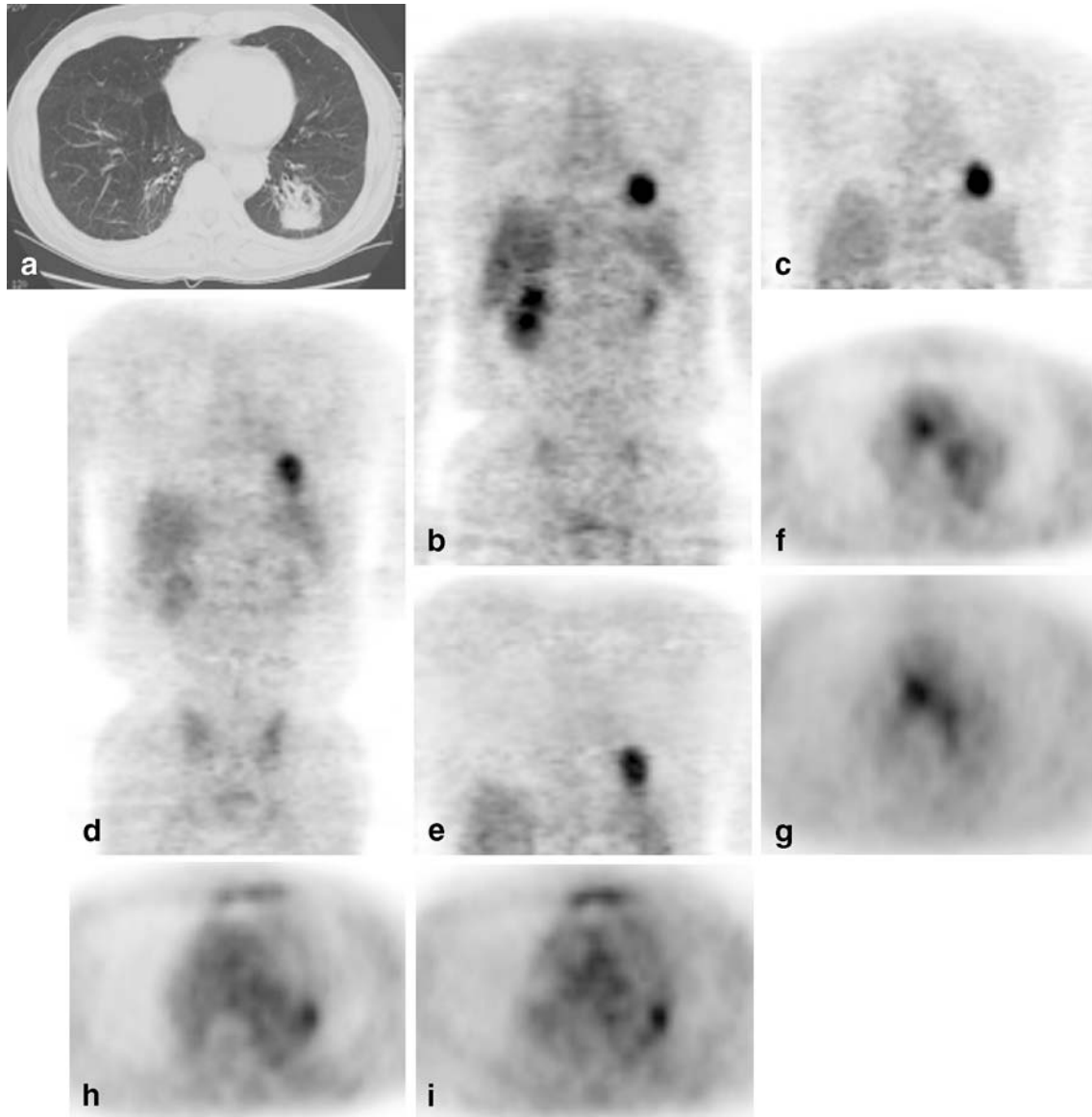
Fig. 4. CT and FDG-PET images of a 73-year-old male pathological non-responder (residual macroscopic disease) with adenocarcinoma in the left lower lobe. CT image before therapy shows a mass shadow in the left lower lobe (**a**). Both early (**b**) and delayed (**c**) FDG-PET coronal images before therapy show intense accumulation in the primary tumour. SUVs for early and delayed images were 6.90 and 9.24, respectively. After chemoradiotherapy, the intense accumulation in the primary tumour was slightly decreased on both early (**d**) and delayed (**e**) FDG-PET coronal images. SUVs for early and delayed images were 4.91 and 5.36, respectively. The percent change values on early and delayed images were 28.8 and 42.0, respectively. Abnormal accumulation in ipsilateral mediastinal (**f** early axial image, **g** delayed axial image) and hilar (**h** early axial image, **i** delayed axial image) lymph nodes was seen after chemoradiotherapy. Nodal stage based on early (**f**, **h**) and delayed (**g**, **i**) FDG-PET images after chemoradiotherapy was N2, but the pathological nodal stage was N1

structures. After induction chemoradiotherapy, nine primary tumours had little or no tumour-related radioactivity whereas 17 primary tumours still had abnormal uptake.

The results in respect of the SUVs in primary tumours are presented in Table 1 and Figs. 1 and 2. The SUVs of the pathological responders decreased significantly after chemoradiotherapy on early and delayed images ($p=0.0002$ and $p=0.0002$, respectively). In the pathological non-responders, there was also a statistically significant decrease on early and delayed images ($p=0.02$ and $p=0.02$, respectively). The differences between SUVs from early images and from delayed images were not significant in either pathological responders or pathological non-responders.

SUV_{after} values from both early and delayed images in pathological responders were significantly lower than those in pathological non-responders ($p=0.0005$ and $p=0.0015$, respectively). SUV_{before} values from both early and delayed images were not significantly different in pathological responders and non-responders.

We found that squamous cell carcinoma had a better response to induction chemoradiotherapy (Table 1). Eighty-six percent (12/14) of patients with squamous cell carcinoma

Table 3. Comparison of the initial clinical nodal stage before induction chemoradiotherapy and the final pathological nodal stage after induction chemoradiotherapy in 26 patients with NSCLC

Clinical stage before induction therapy	Pathological stage after induction therapy		
	N0 (n=18)	N1 (n=3)	N2 (n=5)
N0 (n=3)	3	0	0
N1 (n=4)	3	1	0
N2 (n=18)	11	2	5
N3 (n=1)	1	0	0

were found to be pathological responders, as compared with only 50% (6/12) of patients with adenocarcinoma. However, the SUVs in patients with squamous cell carcinoma did not differ significantly from those in patients with adenocarcinoma among either pathological responders or pathological non-responders.

Taking an arbitrary SUV_{after} of 4.5 as the cut-off for differentiating between pathological responders and non-responders, both early and delayed PET scans showed an overall sensitivity of 88%, a specificity of 89%, a positive predictive value of 78%, a negative predictive value of 94% and an overall accuracy of 89%.

The percent change values calculated from SUV_{before} and SUV_{after} in primary tumours are presented in Table 2. The percent change values from early and delayed images in the pathological responders were significantly higher than those in the pathological non-responders (p=0.003 and p=0.004, respectively). The differences between the percent change values from early images and those from delayed images were not significant in either pathological responders or non-responders. The differences between the percent change in patients with squamous cell carcinoma and that in patients with adenocarcinoma was not statistically significant among either pathological responders or non-responders.

Taking an arbitrary percent change of 65 as the cut-off for differentiating between pathological responders and non-responders, early PET scans had an overall sensitivity of 75%, a specificity of 83%, a positive predictive value of 67%, a negative predictive value of 88% and an overall accuracy of 81%. The corresponding values for delayed

Table 4. Comparison of nodal staging based on FDG-PET scans after induction chemoradiotherapy and pathological findings in 26 patients with NSCLC

FDG-PET stage	Pathological stage		
	N0	N1	N2
N0 (n=21)	18	1	2
N1 (n=1)	0	1	0
N2 (n=4)	0	1	3
Total: 26	18	3	5

PET scans were 63%, 94%, 83%, 85% and 85%, respectively.

Figures 3 and 4 show typical examples of FDG-PET scans in a pathological responder and a non-responder, respectively.

Lymph node restaging after chemoradiotherapy

Of 23 patients with either N1, N2 or N3 disease before induction chemoradiotherapy, 17 were downstaged (Table 3). The results of nodal staging after induction chemoradiotherapy are presented in Table 4. Results from delayed images were exactly the same as those from early images. Overall, the post-chemoradiotherapy PET scan accurately predicted the nodal stage in 22 (85%) of 26 patients. In all 18 patients with pN0 disease, the nodal stage was accurately predicted by preoperative PET scans. Of the eight patients with either pN1 or pN2 disease, five were predicted to be node-positive by PET scan. When the PET scan was evaluated for accuracy in predicting mediastinal nodal involvement only, three of five patients were correctly predicted by PET to have N2 disease.

Discussion

This study demonstrates that FDG-PET was useful in predicting the outcome of preoperative induction chemoradiotherapy in patients with advanced NSCLC. For appropriate decision making in the clinical management of lung cancer patients, there is increasing demand for more sensitive and specific non-invasive imaging procedures for staging and restaging.

One approach currently available to restage lung cancer patients after induction therapy is the performance of repeat CT scans. However, the definition of tumour response using anatomical imaging modalities is based on size criteria. The disease activity may have completely resolved after therapy, but residual masses may persist on morphological imaging as resolution of therapy-induced anatomical changes lag behind tumour cell mortality. As expected, the accuracy of CT scanning in the setting of induction therapy is reported to be quite low [16].

FDG-PET may have wide application in measuring treatment response in oncology. Malignant cells have been shown to have an increased rate of glucose metabolism compared with non-malignant tissue [17]. Residual disease after induction therapy, therefore, would be expected to accumulate FDG and allow patients to be restaged on a physiological basis. Decreased FDG uptake following therapy has been demonstrated with experimental tumour models in animals [18]. Decreased FDG uptake after irradiation is due to reduced numbers of metabolically active tumour cells. It has been suggested that FDG-PET imaging allows differentiation of viable tumour and fibrotic tissue after completion of chemo- and/or radiotherapy [19–21]. In the present study, using threshold values of 4.5 for SUV_{after} and 65% for percent change, we were able to

accurately predict pathological responders with an accuracy of 89% and 81–85%, respectively. FDG-PET also had a high specificity and high negative predictive value. These findings could have significant implications for evaluation of induction chemoradiotherapy response in NSCLC patients. Perhaps, in the future, surgical exploration should be recommended for responders as well as for selected patients with stable disease. If a patient is not responding to the preoperative induction therapy, then a different chemotherapeutic regimen, radiation, or both could be added early in the therapy, thereby significantly reducing the morbidity and costs resulting from ineffective therapy.

Some investigators have concluded, however, that a decrease in FDG uptake does not necessarily indicate a good prognosis [7]. We were not able to make the distinction between residual microscopic disease and pathological complete response. A major limitation of FDG-PET is its poor detection rate for small carcinomas. The current spatial resolution available on modern FDG-PET scanners is usually 4–8 mm. In general, sensitivity is lower for lesions less than 1 cm in diameter, although even very small tumour foci may be identified if their metabolic activity is sufficiently high. In the present study, nine patients had no tumour-related radioactivity after chemoradiotherapy. Of these patients, three had complete pathological response and six had residual microscopic disease. All six residual tumours had microscopic foci of cancer measuring from 0.1 to 5 mm. It is not surprising, therefore, that these tumours could not be visualised.

FDG accumulation after chemoradiotherapy may not always be predictive of the pathological outcome of the primary lesion. The positive predictive value of SUV_{after} and percent change in early images were 78% and 67%, respectively. The required interval for post-therapy evaluation with FDG-PET may be longer for radiotherapy than for chemotherapy. It was reported that FDG uptake in some tumours may not decrease and in fact may even increase after irradiation despite a favourable response in clinical terms [9, 22]. Positive FDG-PET studies after clinically successful radiotherapy have usually been attributed to radiation-induced inflammatory reactions. Reinhardt et al. confirmed that FDG uptake did not differ between viable cancer cells and macrophages [23]. In the post-therapy setting, approximately 25% of FDG uptake can occur in non-tumour tissues such as macrophages, neutrophils, fibroblasts and granulation tissue [24]. To avoid false-positive results due to non-specific treatment effects, the optimal interval from completion of radiotherapy to FDG-PET imaging should be carefully selected. Haberkorn et al. have recommended that in order to completely exclude influences of inflammation, post-therapy FDG-PET studies should be performed at 3–6 months after irradiation [25]. On the other hand, late measurements are confounded by regrowth of tumour cells and do not accurately reflect the status of the tumour after therapy. Presently, there are no systematic data available on patients with NSCLC to determine the optimal time for early metabolic restaging after induction therapy. This needs further studies, including histopathological analysis.

With respect to nodal disease, a report by Gupta et al. demonstrated sensitivity and specificity values of 68% and 61%, respectively, for CT scanning in lung cancer mediastinal lymph node staging, while FDG-PET scanning had a sensitivity and specificity of 87% and 91%, respectively [26]. The critical question in restaging after induction therapy is the presence or absence of residual N2 disease. In the present study, for restaging after chemoradiotherapy, we had only five patients with N2 disease, and FDG-PET scan correctly predicted N2 disease in three of them. The two negative patients had microscopic tumour foci measuring from 1 to 8 mm. A larger study is necessary to confirm the sensitivity and specificity for restaging in the present study. Akhurst et al. found that FDG-PET scanning after induction therapy did not accurately detect the involvement of mediastinal lymph nodes [20]. Lesion detection depends on the size of the tumour deposit and the level of FDG activity in the tumour and surrounding tissues. The microscopic tumour foci that remain after chemoradiotherapy and small tumours surrounded by background soft tissue activity deep in the mediastinum are particularly difficult to detect and may explain the low detectability in our five patients with N2 disease. Minimal lymph node involvement cannot be assessed by any non-invasive method available to date.

It is known that FDG uptake in most malignant tissues increases with time even after 1 h post injection, while that in benign lesions decreases with time [10–14]. Kubota et al. [12] found that delayed FDG-PET imaging detected malignant lesions because of the increased uptake by tumours along with a decreased normal background. Zhuang et al. [10] suggested that lung lesions with decreased or stable SUV over time are likely to have a benign aetiology, whereas those with increased SUV with time are likely to be caused by malignancy. In the present study, we compared early and delayed images to predict response to induction therapy. However, there were no significant differences between the results of early and delayed images. One of the reasons for this may have been the short interval of 1 h between early and delayed acquisitions. Demura et al. reported on the contribution of dual time point images obtained at 1 h and 3 h in patients with lung tumour [14]. Their findings suggested that a longer interval between early and delayed acquisition results in a larger difference in SUV [14]. Thus, it is possible that delaying the delayed scan for an additional 3–4 h may have shown differences in the SUV acquired on early and delayed images that were not observed in the present study. Additionally, SUV is significantly time dependent and further investigation is required with regard to SUV cut-off if more delayed imaging is used. This may have important future implications in terms of treatment monitoring.

Conclusion

Based on the use of threshold values for SUV_{after} and percent change, FDG-PET was found to have high

specificity, negative predictive value and accuracy in predicting the response of the primary tumour to induction chemoradiotherapy. The post-chemoradiotherapy FDG-PET scan accurately predicted nodal stage in 22 of 26 patients. In addition, results of delayed FDG-PET were the same as those of early FDG-PET. These findings suggest that FDG-PET may have a major impact on the design of future therapy monitoring protocols in NSCLC.

References

1. Jemal A, Thomas A, Murray T, Thun M. Cancer statistics. CA Cancer J Clin 2002;52:23–47
2. Martini N, Kris MG, Flehinger BJ, Gralla RJ, Bains MS, Burt ME, et al. Preoperative chemotherapy for stage IIIa (N2) lung cancer: the Sloan-Kettering experience with 136 patients. Ann Thorac Surg 1993;55:1365–73
3. Rusch V, Giroux DJ, Kraut MJ, Crowley J, Hazuka M, Johnson D, et al. Induction chemoradiation and surgical resection for non-small cell lung carcinomas of the superior sulcus: initial results of Southwest Oncology Group Trial 9416 (Intergroup trial 0160). J Thorac Cardiovasc Surg 2001;121:472–83
4. Mac Manus MP, Hicks RJ, Matthews JP, McKenzie A, Rischin D, Salminen EK, et al. Positron emission tomography is superior to computed tomography scanning for response assessment after radical radiotherapy or chemoradiotherapy in patients with non-small cell lung cancer. J Clin Oncol 2003;21:1285–92
5. Valk PE, Pounds TR, Hopkins DM, Haseman MK, Hofer GA, Greiss HB, et al. Staging non-small cell lung cancer by whole-body positron emission tomographic mapping. Ann Thorac Surg 1995;60:1573–82
6. Gambhir SS, Hoh CG, Phelps ME, Madar I, Maddahi J. Decision tree sensitivity analysis for cost-effectiveness of FDG-PET in staging and management of non-small cell lung cancer. J Nucl Med 1996;37:428–36
7. Ichiya Y, Kuwabara Y, Otsuka M, Tahara T, Yoshikai T, Fukumura T, et al. Assessment of response to cancer therapy using fluorine-18-fluorodeoxyglucose and positron emission tomography. J Nucl Med 1991;32:1655–60
8. Hebert ME, Lowe VJ, Hoffman JM, Patz EF, Anscher MS. Positron emission tomography in the pretreatment evaluation and follow-up of non-small cell lung patients treated with radiotherapy: preliminary findings. Am J Clin Oncol 1996;19:416–21
9. Hautzel H, Muller-Gartner HW. Early changes in fluorine-18-FDG uptake during radiotherapy. J Nucl Med 1997;38:1384–6
10. Zhuang H, Pourdehnad M, Lambright ES, Yamamoto AJ, Lanuti M, Li P, et al. Dual time point ^{18}F-FDG PET imaging for differentiating malignant from inflammatory processes. J Nucl Med 2001;42:1412–7
11. Yamada S, Kubota K, Kubota R, Ido T, Tamahashi N. High accumulation of fluorine-18-fluorodeoxyglucose in turpentine-induced inflammatory tissue. J Nucl Med 1995;36:1301–6
12. Kubota K, Itoh M, Ozaki K, Ono S, Tashiro M, Yamaguchi K, et al. Advantage of delayed whole-body FDG-PET imaging for tumour detection. Eur J Nucl Med 2001;28:696–703
13. Matthies A, Hickeson M, Cuchiara A, Alavi A. Dual time point ^{18}F-FDG PET for the evaluation of pulmonary nodules. J Nucl Med 2002;43:871–5
14. Demura Y, Tsuchida T, Ishizaki T, Mizuno S, Totani Y, Ameshima S, et al. ^{18}F-FDG accumulation with PET for differentiation between benign and malignant lesions in the thorax. J Nucl Med 2002;44:540–8
15. Mountain CF, Dresler CM. Regional lymph node classification for lung cancer staging. Chest 1997;111:1718–23
16. Lee K, Shim YM, Han J, Kim J, Ahn YC, Park K, et al. Primary tumors and mediastinal lymph nodes after neoadjuvant concurrent chemoradiotherapy of lung cancer: serial CT findings with pathologic correlation. J Comput Assist Tomogr 2000;24:35–40
17. Pauwels EK, McCready VR, Stoot JH, van Deurzen DF. The mechanism of accumulation of tumor-localizing pharmaceuticals. Eur J Nucl Med 1998;25:277–305
18. Oya N, Nagata Y, Tamaki N, Takagi T, Murata R, Magata Y, et al. FDG-PET evaluation of therapeutic effects on VX2 liver tumor. J Nucl Med 1996;37:296–302
19. Vansteenkiste JF, Stroobants SG, De Leyn PR, Dupont PJ, Verbeken EK. Potential use of FDG-PET scan after induction chemotherapy in surgically staged IIIa-N2 non-small-cell lung cancer: a prospective pilot study—The Leuven Lung Cancer Group. Ann Oncol 1998;9:1193–8
20. Akhurst T, Downey RJ, Ginsberg MS, Gonen M, Bains M, Korst R, et al. An initial experience with FDG-PET in the imaging of residual disease after induction therapy for lung cancer. Ann Thorac Surg 2002;73:259–64
21. Ryu JS, Choi NC, Fischman AJ, Lynch TJ, Mathisen DJ. FDG-PET in staging and restaging non-small cell lung cancer after neoadjuvant chemoradiotherapy: correlation with histopathology. Lung Cancer 2002;35:179–87
22. Fischman AJ, Thornton AF, Frosch MP, Swearinger B, Gonzalez RG, Alpert NM. FDG hypermetabolism associated with inflammatory necrotic changes following radiation of meningioma. J Nucl Med 1997;38:1027–9
23. Reinhardt MJ, Kubota K, Yamada S, Iwata R, Yaegashi H. Assessment of cancer recurrence in residual tumors after fractionated radiotherapy: a comparison of fluorodeoxyglucose, L-methionine and thymidine. J Nucl Med 1997;38:280–7
24. Kubota R, Yamada S, Kubota K, Ishiwata K, Tamahashi N, Ido T. Intratumoral distribution of F-18-fluoro-deoxyglucose in vivo: high accumulation in macrophages and granulation tissues studied by micro-autoradiography. J Nucl Med 1992;33:1972–80
25. Haberkorn U, Strauss LG, Dimitrakopoupou A, Engenhart R, Oberdorfer F, Ostertag H, et al. PET studies of fluorodeoxyglucose metabolism in patients with recurrent colorectal tumors receiving radiotherapy. J Nucl Med 1991;32:1485–90
26. Gupta NC, Tamim WJ, Graeber GG, Bishop HA, Hobbs GR. Mediastinal lymph node sampling following positron emission tomography with fluorodeoxyglucose imaging in lung cancer staging. Chest 2001;120:521–7